

Article

The Single-Step Fabrication of a Poly (Sodium Vinylsulfonate)-Grafted Polyetheretherketone Surface to Ameliorate Its Osteogenic Activity

Lvhua Liu ^{1,†}, Jun Dong ^{1,†}, Weifang Zhang ², Chanjuan He ², Ying Liu ² and Yanyan Zheng ^{1,*} 

¹ School of Pharmacy, North Sichuan Medical College, Nanchong 637100, China; mosheng1025@163.com (L.L.); dongj46@163.com (J.D.)

² Department of Stomatology, North Sichuan Medical College, Nanchong 637100, China; flory1974@126.com (W.Z.); hechanjuan0615@163.com (C.H.); ying_nsmc@hotmail.com (Y.L.)

* Correspondence: yanyzheng@163.com

† These authors contributed equally to this work.

Abstract: Polyetheretherketone (PEEK) is considered a potential material for replacing traditional biomedical metals used in orthopedic implants because of its similar elastic modulus to human bone. However, the poor osteogenic activity of PEEK itself hinders its clinical application. In this study, a PEEK surface was grafted with poly (sodium vinylsulfonate) through a single-step ultraviolet-initiated graft polymerization method to ameliorate its osteogenic activity. X-ray photoelectron spectroscopy and water contact angle measurements confirmed that different amounts of poly (sodium vinylsulfonate) were grafted onto the PEEK surface upon varying the ultraviolet irradiation time. Atomic force microscopy revealed that the surface topography and roughness of PEEK before and after surface grafting did not change significantly. The in vitro results showed that grafting with poly (sodium vinylsulfonate) rendered the PEEK surface with improved MC3T3-E1 osteoblast compatibility and osteogenic activity. Moreover, a PEEK surface with a higher grafting amount of poly (sodium vinylsulfonate) was observed to be more beneficial to the proliferation and osteogenic differentiation of MC3T3-E1 osteoblasts. Collectively, by employing this simple and one-step method, the osteogenic activity of PEEK can be enhanced, paving the way for the clinical application of PEEK in orthopedic implants.

Keywords: polyetheretherketone; poly (sodium vinylsulfonate); osteogenic activity; ultraviolet-initiated graft polymerization; osseointegration



Citation: Liu, L.; Dong, J.; Zhang, W.; He, C.; Liu, Y.; Zheng, Y. The Single-Step Fabrication of a Poly (Sodium Vinylsulfonate)-Grafted Polyetheretherketone Surface to Ameliorate Its Osteogenic Activity. *Coatings* **2022**, *12*, 868. <https://doi.org/10.3390/coatings12060868>

Academic Editor: Soo-Hwan Byun

Received: 11 April 2022

Accepted: 17 June 2022

Published: 20 June 2022

Publisher's Note: MDPI stays neutral with regard to jurisdictional claims in published maps and institutional affiliations.



Copyright: © 2022 by the authors. Licensee MDPI, Basel, Switzerland. This article is an open access article distributed under the terms and conditions of the Creative Commons Attribution (CC BY) license (<https://creativecommons.org/licenses/by/4.0/>).

1. Introduction

Artificial orthopedic substitutes show great potential to treat irreparable bone destruction. With respect to the clinical applications, rapid and efficient osseointegration between the extraneous implant surface and the host bone tissue is pivotal [1,2]. Compared with traditional metals (e.g., titanium and its alloys, etc.), the elastic modulus of polyetheretherketone (PEEK) is analogous to that of human bone [3–5]. An analogous modulus can reduce the stress-shielding effect resulting from the elastic modulus mismatch between the extraneous implant and host bone, preventing potential peri-implant osteonecrosis and bone resorption. In addition, PEEK possesses many favorable attributes, including exceptional chemical and sterilization resistance, natural radiolucency, and suitable mechanical strength. Consequently, PEEK is considered an alternative to biomedical metal in orthopedic implants [6]. However, despite these fascinating features, the poor osteogenic ability of PEEK itself hinders its interfacial interaction with bone tissue limiting its clinical use as an orthopedic implant [4,7].

Poor osteogenic activity results in insufficient bone–implant integration, leading to loosening and, eventually, the complete failure of implants. Therefore, to achieve optimal

osseointegration and intended implant function, it is important to endow implants with improved osteogenic activity. Currently, two main strategies are being developed to speed up the osseointegration of PEEK: bioactive composite preparation and surface modification [8]. Bioactive ceramic components (e.g., calcium silicate, hydroxyapatite and bioactive glass, etc.) are usually added to the PEEK substrate to improve its osteogenic activity [9–11]. However, during the preparation of bioactive PEEK composites, the mechanical properties are compromised by enhancing their osteogenic activity. The surface properties of the implants play a crucial role in bone–implant integration [12]. Surface modification provides favorable physical and chemical properties to the implant surface, enhancing its osteogenic activity, and does not diminish the beneficial properties of bulk materials. Thus, the PEEK surface was coated with bioactive ceramic using various coating techniques, such as electron beam evaporation [13], thermal plasma spraying [14], microwave-assisted deposition [15] and spin spray [16], and biomimetics [17]. However, for the bioactive ceramic coating on the PEEK surface, severe inflammation and bone resorption may be induced by ceramic particles produced by shedding or abrasion [18].

Chemical modification of implants surface can overcome these shortcomings. However, it is difficult to functionalize the PEEK surface through chemical reactions because of its resonance-stabilized chemical structure. Nevertheless, Kassick et al. developed a mild covalent surface modification approach through the acid-mediated addition of oxyamine and hydrazine nucleophiles to the diaryl ketone moiety of PEEK to enhance its osteoconduction [19]. Zheng et al. first reduced the carbonyl groups in the diaryl ketone moiety of PEEK to hydroxyl groups and formed a silanization layer on the hydroxylation-pretreated PEEK surface. Finally, $-\text{COOH}$, $-\text{OH}$, and $-\text{PO}_4\text{H}_2$ groups and GRGD peptides were introduced onto the PEEK surface by further tailoring the silanization layer [20,21]. However, these methods are often time-consuming and require multiple steps. Thus, it is important to develop simple and effective strategies for the functionalization of PEEK surfaces to enhance their osteogenic activity.

Photo-induced grafting offers many advantages over other methods (e.g., plasma- and radiation-induced grafting, etc.), for instance, simple equipment, low cost, mild reaction conditions, easy to industrialize, and durable chemical stability of the grafted polymers [22]. The diaryl ketone moiety of PEEK is analogous to that of the photoinitiator, benzophenone. A previous study showed that the diaryl ketone moiety of PEEK transforms into a semi-benzopinacol radical upon exposure to ultraviolet (UV) irradiation [23]. The radicals initiate the grafting polymerization of functional monomers on the PEEK surface. Thus, the functional polymer layer was covalently grafted onto the PEEK surface through the simple and single-step UV-induced graft polymerization method. The grafting of functional monomers such as acrylic acid, 2-methacryloyloxyethyl phosphorylcholine, 3-sulfopropyl methacrylate potassium salt, and monomethoxy terminated oligo(ethylene glycol) methacrylate on the surface of PEEK has been achieved using UV-initiated graft polymerization [24–26]. Moreover, our previous studies also used UV-induced graft polymerization to successfully graft poly (vinylphosphonic acid), poly(sodium *p*-styrenesulfonate), and poly (sodium vinylsulfonate) on the surface of PEEK [27–30]. The functional PEEK showed enhanced osteogenic activity *in vitro* and improved osseointegration ability *in vivo*.

The purpose of this study was to obtain the optimal poly (sodium vinylsulfonate)-grafted PEEK implants. Thus, in the present study, poly (sodium vinylsulfonate) was grafted onto the surface of PEEK through a single-step and simple UV-induced graft polymerization method and different amounts of poly (sodium vinylsulfonate)-grafted PEEK were obtained by changing the time of UV irradiation. Furthermore, the effect of the amount of poly (sodium vinylsulfonate) on the osteogenic activity of MC3T3-E1 osteoblasts was systematically evaluated to determine the optimal poly (sodium vinylsulfonate)-grafted PEEK implants.

2. Materials and Methods

2.1. Materials

PEEK discs ($\Phi 15 \text{ mm} \times 1 \text{ mm}$) were obtained from JUNHUA chinaPEEK (Changzhou, China). Sodium vinylsulfonate was obtained from TCI Development Co., Ltd. (Shanghai, China).

2.2. Sample Preparation

Before grafting, the samples were ultrasonically rinsed with acetone, ethanol, and deionized water in sequence and dried at room temperature. The poly (sodium vinylsulfonate)-grafted PEEK surfaces were prepared as previously reported [30]. Briefly, PEEK specimens were soaked in a 1.0 M sodium vinylsulfonate deionized water solution, and then the solution was irradiated with UV light (maximum intensity at 365 nm) to trigger the graft polymerization reaction. The reaction was conducted for 20 min, 40 min, or 90 min. Then, the grafted specimens were ultrasonically rinsed in deionized water to remove residual monomers and nongrafted homopolymers. The functional PEEK samples were dried at room temperature and labeled as PESA20, PESA40, and PESA90.

2.3. Characterization

The surface chemical composition of the untreated PEEK and PESA samples was detected by X-ray photoelectron spectroscopy (XPS, AXIS Ultra, Kratos Analytical, Manchester, UK) with Al K α radiation. The sample charging was calibrated to the reference C1s set at 284.8 eV. Deconvolution into subpeaks was performed using the least-squares peak analysis software XPS PEAK95 Version 3.1 and the Lorentzian–Gaussian sum function.

The surface wettability of the untreated PEEK and PESA samples was determined by a contact angle goniometer (Krüss DSA100, Hamburg, Germany). A 3 μL deionized water droplet was dropped on the sample surface using a motor-driven syringe, and four samples per group were measured.

Atomic force microscopy (AFM; Dimension icon, Bruker, Santa Barbara, CA, USA) observation was conducted to study the surface topography of the untreated PEEK and PESA specimens. The scan range was $20 \mu\text{m} \times 20 \mu\text{m}$, and NanoScope Analysis software was used to obtain average roughness (Ra).

The grafting amount of poly (sodium vinylsulfonate) was calculated according to the following equation:

$$\text{The grafting amount of poly (sodium vinylsulfonate) (mg/cm}^2\text{)} = (W_1 - W_0)/S.$$

Where W_1 is the weight of PEEK with poly (sodium vinylsulfonate), W_0 is the weight of PEEK, and S is the specimen surface area.

2.4. Cell Culture

Mouse MC3T3-E1 osteoblasts were obtained from the cell bank of the Chinese Academy of Sciences (Shanghai, China). MC3T3-E1 osteoblasts were cultured in α -MEM (HyClone) containing 10% fetal bovine serum (HyClone) and 1% penicillin/streptomycin (HyClone) at 37 °C in a humidified atmosphere of 5% CO₂. Except where otherwise noted, the samples were placed in a 24-well plate, and the inoculum density of MC3T3-E1 osteoblasts on the samples was 1×10^4 cells/well. For osteogenic induction, an osteogenic induction medium containing 100 nM dexamethasone (Sigma, St. Louis, MO, USA), 10 mM β -glycerophosphate (Sigma), and 50 $\mu\text{g/mL}$ ascorbic acid (Sigma) was used when the MC3T3-E1 osteoblasts cultured on the samples reached 85% confluence. The medium was changed every three days. All samples were sterilized with epoxy ethane before cell seeding.

2.5. Cell Attachment and Proliferation

The attachment and proliferation of MC3T3-E1 osteoblasts were evaluated using the 3-(4,5-dimethylthiazol-2-yl)-2,5-diphenyltetrazolium bromide (MTT, Sigma) assay [31]. For the attachment assay, 1.0×10^5 cells were cultured on each sample for 4 h. For the

proliferation evaluation, 1.0×10^4 cells were seeded on each sample for 1, 4, and 7 d. At a scheduled time, the specimens were rinsed thrice with sterile phosphate-buffered saline (PBS) and then incubated in a 1 mL α -MEM solution containing 40 μ L MTT (5 mg/mL in PBS). After incubation for 4 h at 37 °C, 500 μ L of dimethyl sulfoxide was used to dissolve insoluble formazan crystals. Finally, 200 μ L of the medium was carefully transferred to a 96-well plate, and a microplate reader (SpectraMax M2, Molecular Devices, Sunnyvale, CA, USA) was used to measure the optical density (OD) at 490 nm.

2.6. Cell Morphology

After seeding 2.0×10^4 cells on each sample and incubating for 4 and 24 h, the morphologies of the MC3T3-E1 osteoblasts were observed by scanning electron microscopy (SEM, Hitachi S-4200, Tokyo, Japan). Briefly, the medium was removed at a predetermined time. Sterile PBS and 2.5% glutaraldehyde were added to rinse the specimens and to fix the osteoblast at 4 °C overnight, respectively. Then, the fixed osteoblasts were subjected to step dehydration with graded ethanol solutions of 30, 50, 70, 90, 95, and 100% for 15 min each. Finally, the morphologies of osteoblasts on the sample's surface were examined by SEM after being sputter-coated with gold.

2.7. Osteogenic Activity Studies

2.7.1. Alkaline Phosphatase (ALP) Activity

After osteogenic induction for 7 and 14 d, the specimens were rinsed thrice with sterile PBS, and then the cells were lysed using RIPA lysis buffer (Beyotime, Shanghai, China) at 4 °C for 40 min. The cell lysis solution was centrifuged at 14,000 rpm for 10 min at 4 °C, and the supernatant was extracted for the ALP activity assay using an ALP assay kit (Nanjing Jiancheng Bioengineering Institute, Nanjing, China) following the manufacturer's protocols. The total protein content was measured using a bicinchoninic acid protein assay kit (Nanjing Jiancheng Bioengineering Institute). The ALP activity of the samples was standardized using the corresponding protein content.

2.7.2. Extracellular Matrix (ECM) Mineralization

The degree of ECM mineralization was evaluated by alizarin red staining. After osteogenic induction for 7 and 14 d, MC3T3-E1 cells on specimens were rinsed thrice with sterile PBS and fixed with 75% ethanol for 1 h. Then, Alizarin Red water solution (pH = 4.2) was added and incubated for 10 min at room temperature. Subsequently, excess Alizarin Red was removed with deionized water. For quantitation, 10% cetylpyridinium chloride (Sigma) in 10 mM sodium phosphate (pH = 7.0) was added to elute adsorbed Alizarin Red on the samples. The absorbance of the eluant was detected by a microplate reader at 620 nm.

2.7.3. Collagen Secretion

On the specimens, collagen secretion was tested by quantifying MC3T3-E1 osteoblast using Sirius Red staining. After osteogenic induction for 7 and 14 d, MC3T3-E1 cells on specimens were rinsed thrice with sterile PBS and fixed in 4% paraformaldehyde. Then, 0.1% Sirius Red (Sigma) solution in saturated picric acid was added and incubated for 18 h at room temperature. Subsequently, 0.1 M acetic acid was used to remove excess Sirius Red. For quantitation, eluent (0.2 M NaOH/methanol = 1:1) of 500 μ L was added to elute adsorbed Sirius Red. Additionally, a microplate reader was used to detect the absorbance of the eluant at 540 nm.

2.7.4. Osteogenesis-Related Genes Expressions

Real-time quantitative PCR (RT-qPCR) analysis was used to evaluate the expression of osteogenesis-related genes, including ALP, osteocalcin (OCN), osteopontin (OPN), and bone morphogenetic protein 2 (BMP-2). After osteogenic induction for 7 and 14 d, the samples were washed thrice with sterile PBS. Whole RNA was extracted from MC3T3-E1

osteoblasts using the TRIZOL reagent (Invitrogen, Carlsbad, CA, USA), and 1 ug total RNA was translated into cDNA using a reverse transcription kit (Takara) according to the manufacturer's instructions. A CFX Connect Real-Time PCR System (Bio-Rad, Hercules, CA, USA) was used for qPCR analysis using the following procedures: denaturation at 95 °C for 10 min and 40 cycles of PCR (95 °C for 15 s and 60 °C for 1 min). The relative gene expression levels were calculated using the $2^{-\Delta\Delta C_t}$ method with CT (cycle threshold) values normalized to the housekeeping gene β -actin. The forward and reverse primers employed in this study are listed in Table 1.

Table 1. Primer sequences used for RT-qPCR analysis.

Gene	Primers
ALP	Forward: CTCCATCTTTGGTCTGGCTCC Reverse: CCTGGTAGTTGTTGTGAGCGTAAT
OCN	Forward: TGGCTGCGCTCTGTCTCTCT Reverse: TTCACTACCTTATTGCCCTCCTG
OPN	Forward: TAGGAGTTTCCAGGTTTCTGATGA Reverse: CTGCCCTTTCCGTTGTTGTC
BMP-2	Forward: GACATCCGCTCCACAAACGA Reverse: CATCACTGAAGTCCACATACAAAGG
β -actin	Forward: AGATTACTGCTCTGGCTCCTAGC Reverse: ACTCATCGTACTCCTGCTTGCT

2.8. Statistical Analysis

One-way ANOVA followed by least significant difference post hoc tests were used to identify statistical significance using SPSS 16.0. Statistical significance was set at $p < 0.05$.

3. Results and Discussion

3.1. Characterization

To corroborate the successful grafting of poly (sodium vinylsulfonate) onto the surface of the PEEK substrates, PEEK, PESA20, PESA40, and PESA90 samples were first characterized by XPS. Figure 1 show the XPS survey spectra and the corresponding high-resolution S2p spectra of PEEK, PESA20, PESA40, and PESA90. Only the C1s and O1s peaks were observed from the untreated PEEK surface, indicating the PEEK surface was free of contamination. Compared with the untreated PEEK surface, new S2p and S2s peaks were detected on the PESA20, PESA40, and PESA90 surfaces. The detection of S can be ascribed to the sulfonate groups in the grafting poly (sodium vinylsulfonate). Furthermore, the high-resolution S2p spectra for PESA20, PESA40, and PESA90 showed two major peaks at 168.3 eV for S2p_{3/2} and 169.4 eV for S2p_{1/2}, indicating that the high-oxidation state sulfonate groups were detected on the sample's surface [29]. The grafting amount of poly (sodium vinylsulfonate) was evaluated by the mass variation of PEEK before and after surface grafting relative to the surface area, and the results are presented in Figure 2a. From the results, we could conclude that the grafting amount of poly (sodium vinylsulfonate) progressively increased as the photo-induced graft polymerization time increased. The results of the atomic percentage and the S/C ratio obtained using XPS analysis for PEEK, PESA20, PESA40, and PESA90 are shown in Figures 2b and 2c, respectively. The variation of S percentage (Figure 2b) and the S/C ratio (Figure 2c) also indirectly indicated the grafting amount of poly (sodium vinylsulfonate) increased with increasing the photo-induced graft polymerization time. Thus, these results indicated that different amounts of poly (sodium vinylsulfonate) were successfully grafted onto the PEEK surface.

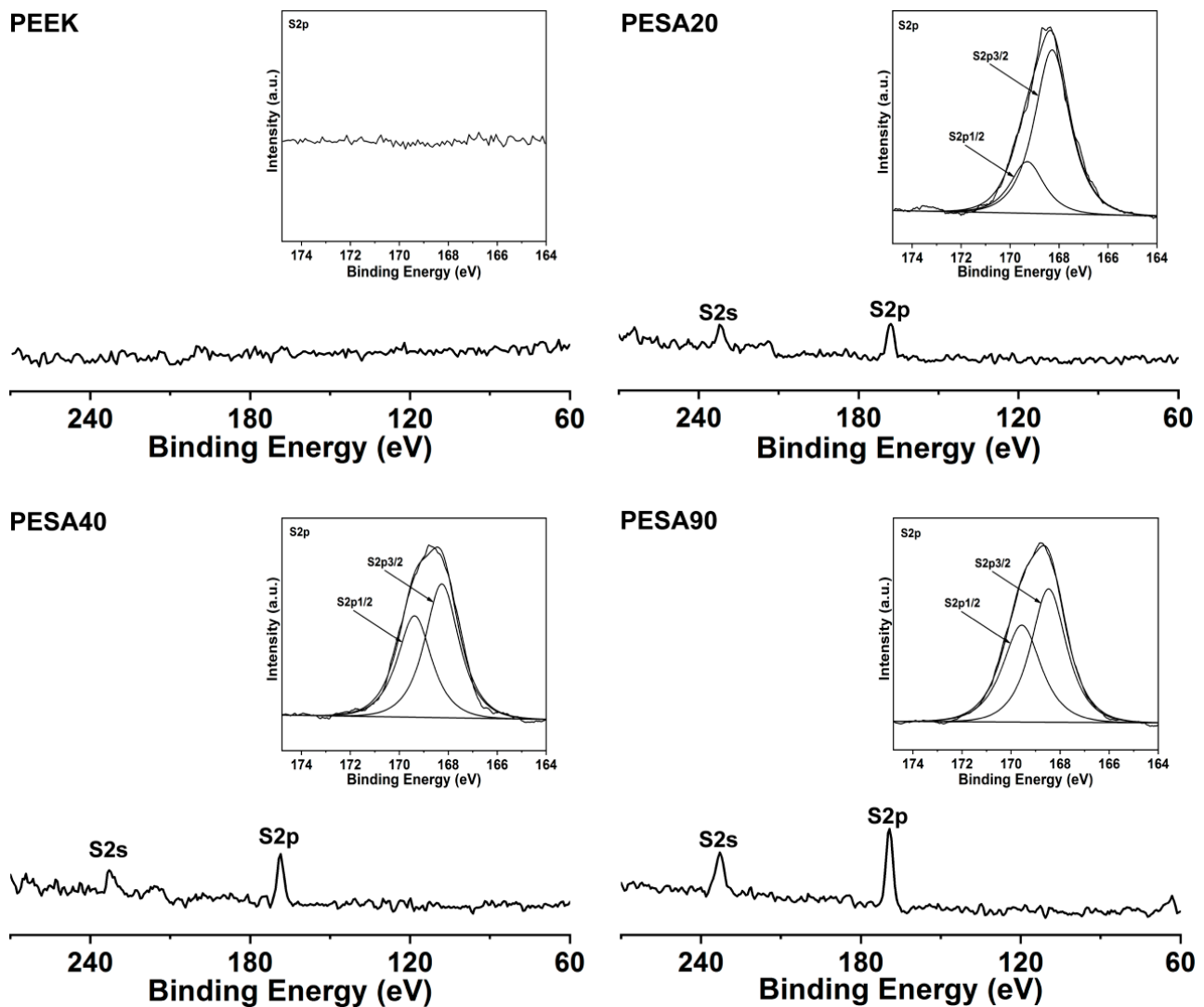


Figure 1. XPS survey spectra and the corresponding S2p high-resolution XPS spectra of PEEK, PESA20, PESA40, and PESA90.

Surface wettability regulates cell behavior on the material surface. Previous studies have suggested that cell adhesion, proliferation, and osteogenic differentiation on the hydrophilic surface are better than that on the hydrophobic surface [32,33]. Thus, the surface hydrophilicity of PEEK, PESA20, PESA40, and PESA90 were characterized (Figure 3). The water contact angle of PEEK was 87.2° , whereas that of PESA20, PESA40, and PESA90 decreased to 56.6° , 42.4° , and 30.7° , respectively, indicating that the surface became more hydrophilic after grafting the hydrophilic polymer poly (sodium vinylsulfonate) on the surface of PEEK. In addition, the gradually decreasing contact angle from PESA20 to PESA40 and PESA90 indicates that the grafting content of poly (sodium vinylsulfonate) on the PEEK surface gradually increases. Thus, the hydrophilic PEEK surface obtained by grafting poly (sodium vinylsulfonate) was expected to be favorable for osteoblast adhesion, proliferation, and osteogenic differentiation.

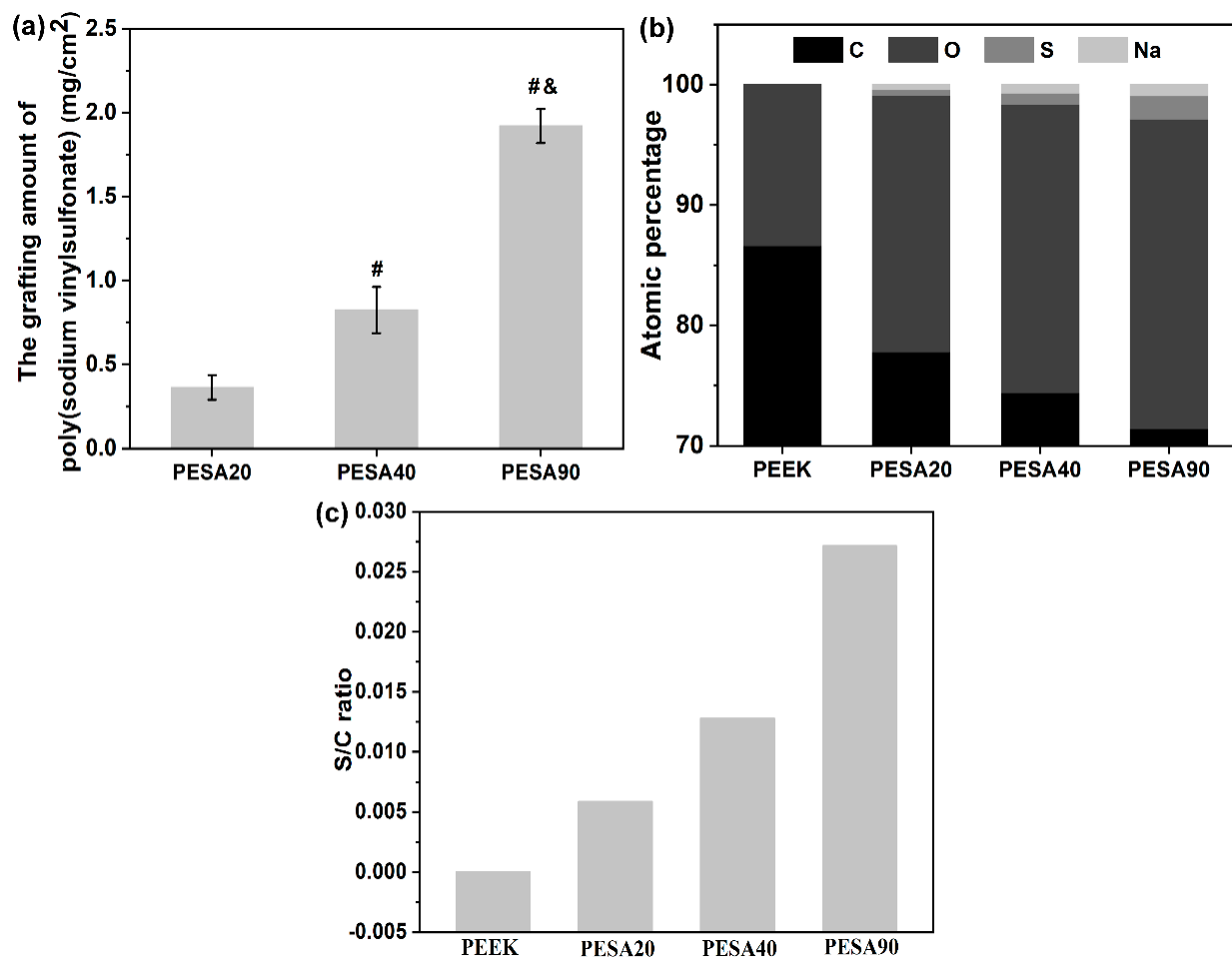


Figure 2. The grafting amount of poly (sodium vinylsulfonate) (a) calculated by the mass variation of PEEK before and after surface grafting relative to surface area. Atomic percentage (b) and S/C ratio (c) obtained from XPS results for PEEK, PESA20, PESA40, and PESA90. Statistically significant differences were indicated by # $p < 0.05$ compared with the PESA20 and & $p < 0.05$ compared with the PESA40. All data represent the mean value \pm standard deviation ($n = 3$ per group).

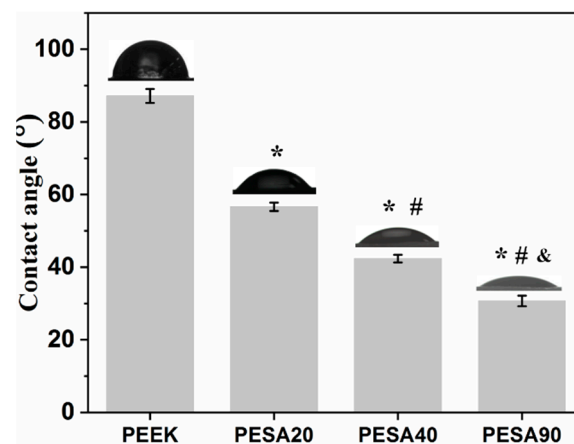


Figure 3. Water contact angles of PEEK, PESA20, PESA40, and PESA90. Statistically significant differences were indicated by * $p < 0.05$ compared with the PEEK, # $p < 0.05$ compared with the PESA20 and & $p < 0.05$ compared with the PESA40. All data represent the mean value \pm standard deviation ($n = 4$ per group).

Surface topographical features, including surface patterns and roughness of the implant surface, can direct the biophysical and biochemical signaling pathways involved in cell responses to the material surface [12]. Thus, the surface topographical parameters of the PEEK, PESA20, PESA40, and PESA90 samples were characterized by AFM. As shown in Figure 4, PEEK, PESA20, PESA40, and PESA90 showed similar topographical patterns. In addition, the PESA20, PESA40, and PESA90 samples had similar Ra values (approximately 21.9 nm) to those of ungrafted PEEK (23.1 nm). These results indicate that the surface grafting of poly (sodium vinylsulfonate) on PEEK does not significantly alter the surface topographical features. Consequently, the difference in the osteoblast responses to untreated PEEK and surface-grafted PEEK can be ascribed to the surface-grafted poly (sodium vinylsulfonate).

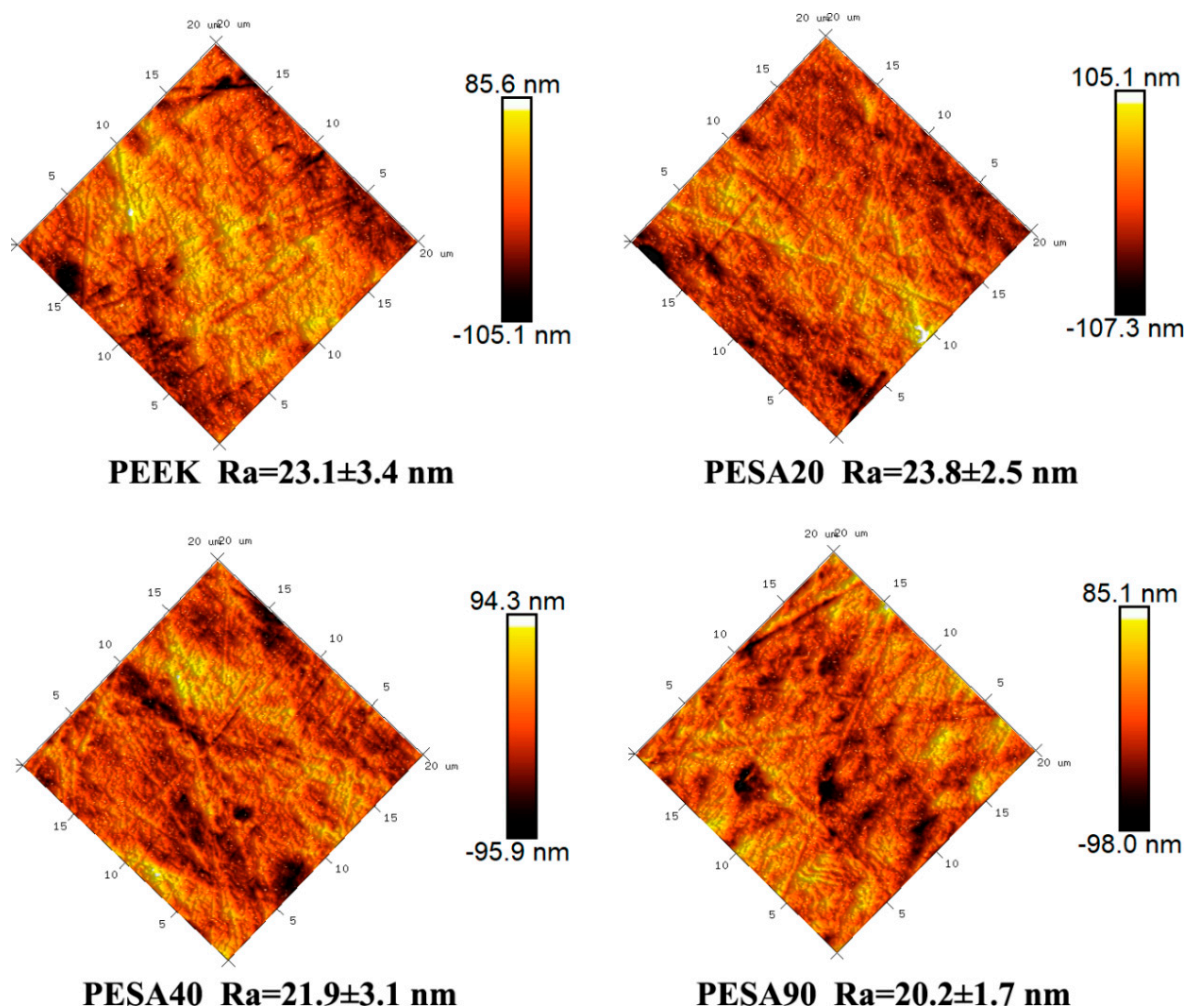


Figure 4. Surface morphology and the corresponding Ra roughness were determined using AFM of PEEK, PESA20, PESA40, and PESA90. All data represent the mean value \pm standard deviation ($n = 3$ per group).

3.2. MC3T3-E1 Osteoblast Responses

The initial adhesion and spreading of osteoblasts cultured on the biomaterial surface play a central role in their subsequent capacity for proliferation and differentiation. Thus, the morphologies of MC3T3-E1 osteoblasts were first monitored using SEM after culturing for 4 and 24 h, as shown in Figure 5. Spherical cells with few pseudopods were observed on the PEEK surface, indicating poor adhesion during the initial 4 h of inoculation, whereas the cells on PESA20, PESA40, and PESA90 surfaces exhibited flat morphologies with apparent filopodia extensions. After 24 h of culture, the MC3T3-E1 osteoblasts showed a slightly

spreading morphology on the surface of PEEK, whereas those on the PESA20, PESA40, and PESA90 surfaces fully spread out. Additionally, MC3T3-E1 osteoblasts were more interconnected through filopodia and lamellipodia on the poly (sodium vinylsulfonate)-grafted PEEK surface, particularly on the surface with a higher grafting amount of poly (sodium vinylsulfonate).

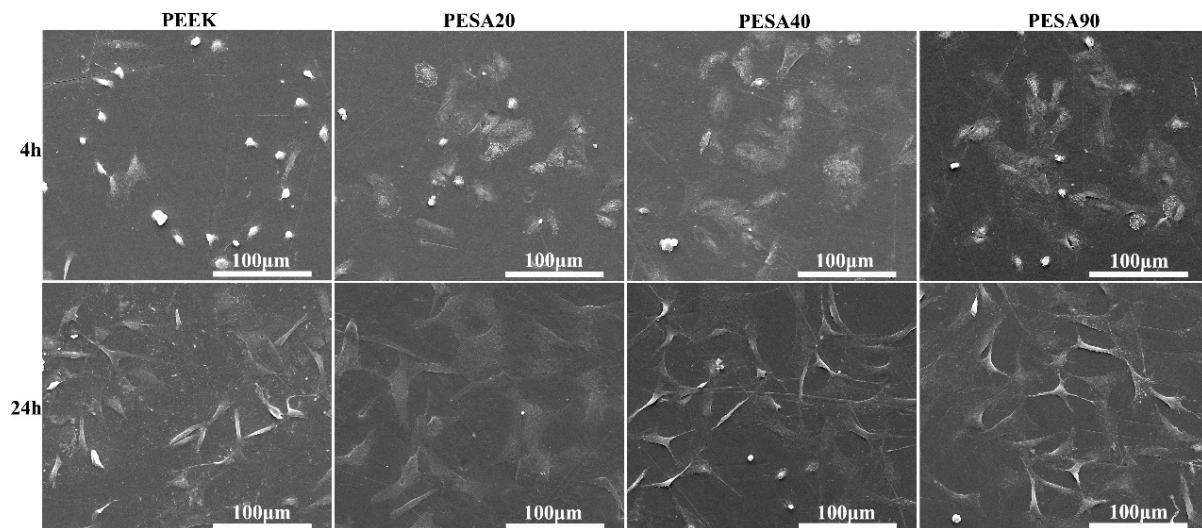


Figure 5. The morphology of MC3T3-E1 osteoblast on different samples after 4 and 24 h of culture.

Figure 6a show the quantitative analysis results of cell adhesion on the untreated and poly (sodium vinylsulfonate)-grafted PEEK sample surfaces. More MC3T3-E1 osteoblasts attached to the poly (sodium vinylsulfonate)-grafted PEEK sample surfaces after culturing for 4 h than to PEEK ($p < 0.05$), indicating that surface grafting of poly (sodium vinylsulfonate) could improve the adhesion of MC3T3-E1 osteoblasts. In addition, the number of adherent cells on PESA90 was higher than that on PESA20 and PESA40. Osteoblast proliferation is fundamental for in vivo bone regeneration [34]. Herein, the time-related proliferation of MC3T3-E1 osteoblasts was measured using an MTT assay. The results (Figure 6b) showed that MC3T3-E1 osteoblasts on the surfaces of different samples exhibited good proliferation activity during the culture period. Compared with the bare PEEK group, more MC3T3-E1 osteoblasts were observed on the PESA20, PESA40, and PESA90 substrates, especially on the PESA90 samples. Overall, the above results indicate that the poly (sodium vinylsulfonate)-grafted PEEK surface displayed better cytocompatibility.

The in vitro osteogenic activity of MC3T3-E1 osteoblasts grown on untreated and poly (sodium vinylsulfonate)-grafted PEEK samples were evaluated in terms of ALP activity, ECM mineralization, and collagen secretion. The ALP expression level of MC3T3-E1 osteoblasts seeded on various substrates is shown in Figure 7a. The ALP activity of MC3T3-E1 osteoblasts on different samples followed the trend PEEK < PESA20 < PESA40 < PESA90 on both days 7 and 14. A similar trend in the quantitative results of ECM mineralization (Figure 7b) and collagen secretion (Figure 7c) was observed at both 7 and 14 d. ALP activity is an early marker of the osteogenic differentiation of osteoblasts. ECM mineralization is considered to be a later marker of the osteogenic differentiation of osteoblasts. COL is a major component of the ECM. Thus, the results indicate that the MC3T3-E1 osteoblasts seeded on the poly (sodium vinylsulfonate)-grafted PEEK surface exhibited better osteogenic activity in the early and late stages of cell culturing than those on the untreated PEEK surface. To further assess the osteogenic differentiation activity of MC3T3-E1 osteoblasts grown on different samples surface at the gene level, the expression of osteogenesis-related genes (ALP, OPN, OCN, and BMP-2) was detected by RT-qPCR. As shown in Figure 8, four osteogenesis marker genes in MC3T3-E1 osteoblasts seeded on PESA20, PESA40, and PESA90 substrates surface were upregulated compared to those in the intact PEEK control

after culturing for 7 and 14 d. MC3T3-E1 osteoblasts grown on the PESA90 samples had the highest expression of ALP, OPN, OCN, and BMP-2 among all the groups. Thus, the RT-qPCR results confirmed that poly (sodium vinylsulfonate)-grafted PEEK surface could boost the osteogenic differentiation of MC3T3-E1 osteoblasts.

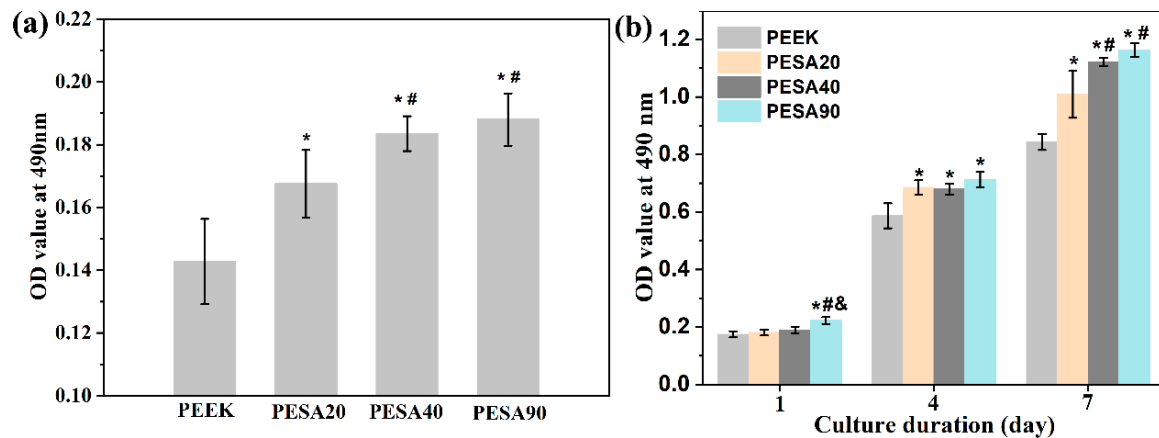


Figure 6. The results of MC3T3-E1 osteoblast adhesion (a) and proliferation (b) on different samples measured using MTT after 4 h, and 1, 4, and 7 d of culture. Statistically significant differences were indicated by * $p < 0.05$ compared with the PEEK, # $p < 0.05$ compared with the PESA20 and & $p < 0.05$ compared with the PESA40. All data represent the mean value \pm standard deviation ($n = 4$ per group).

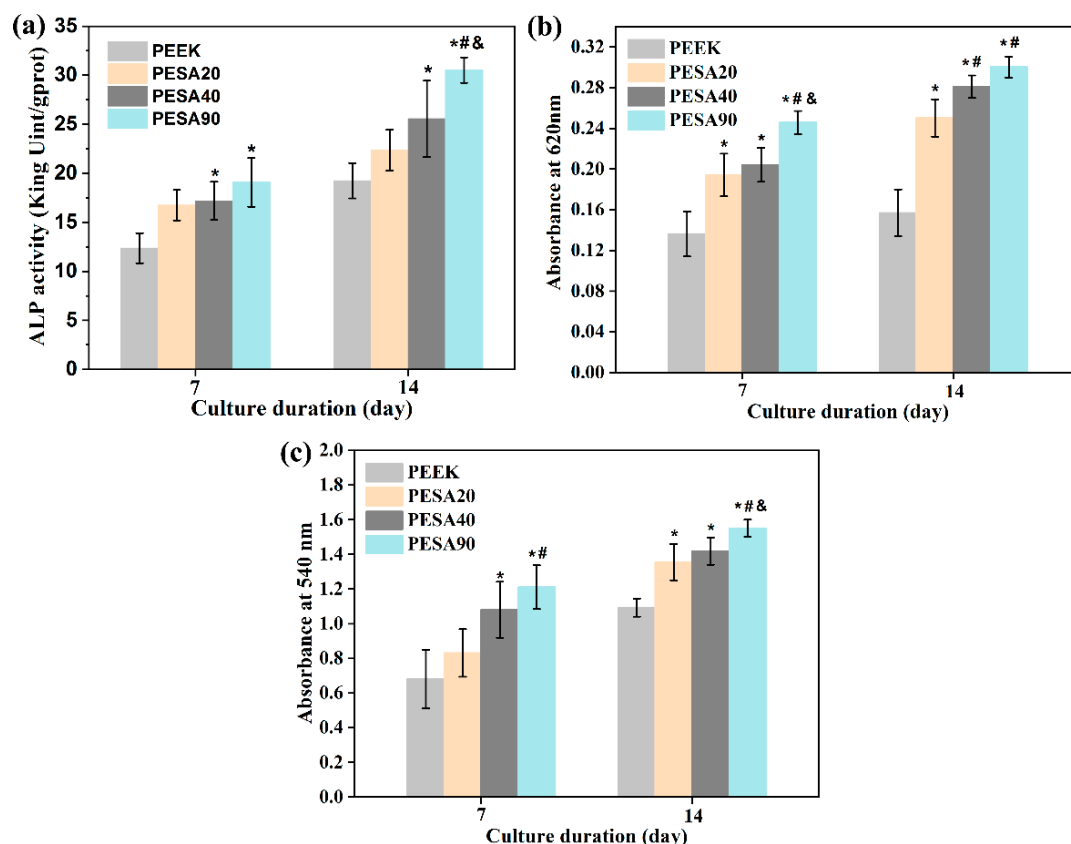


Figure 7. The quantitative results of (a) ALP activity, (b) ECM mineralization, and (c) COL secretion at different time points (days 7 and 14). Statistically significant differences were indicated by * $p < 0.05$ compared with the PEEK, # $p < 0.05$ compared with the PESA20, and & $p < 0.05$ compared with the PESA40. All data represent the mean value \pm standard deviation ($n = 4$ per group).

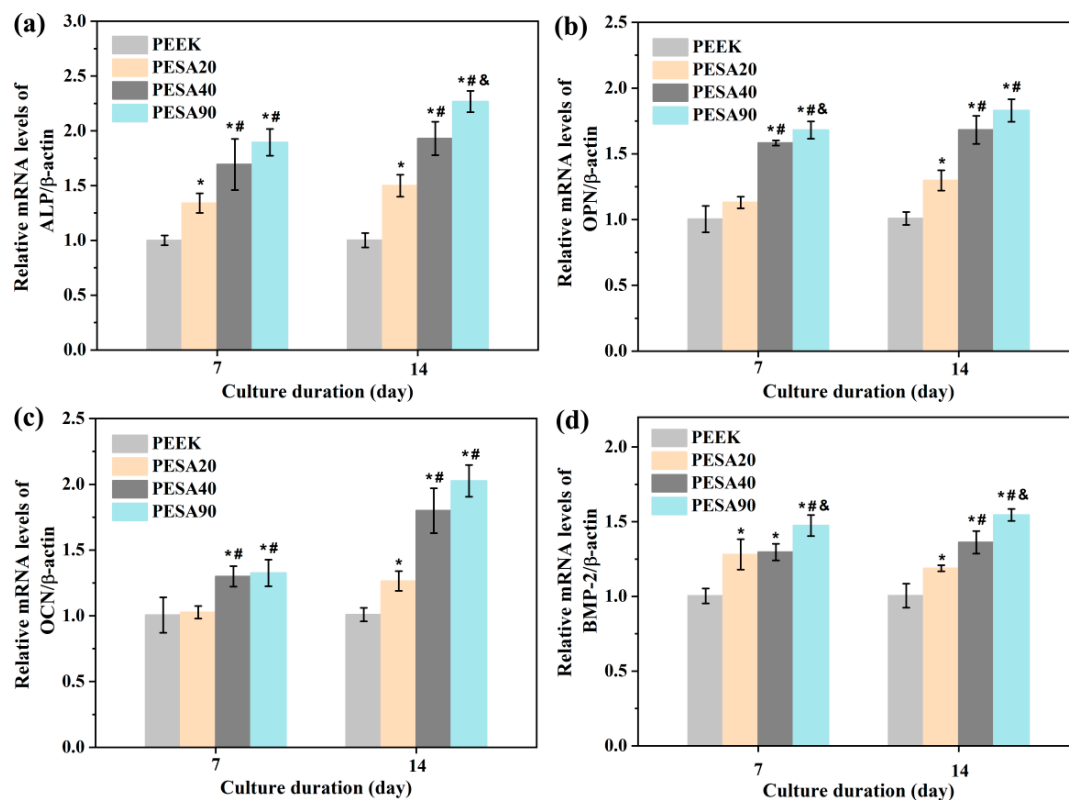


Figure 8. Osteogenic gene expression of MC3T3-E1 osteoblasts cultured on different samples at different time points (days 7 and 14) determined using RT-qPCR: (a) ALP, (b) OPN, (c) OCN, and (d) BMP-2. Statistically significant differences were indicated by * $p < 0.05$ compared with the PEEK, # $p < 0.05$ compared with the PESA20, and & $p < 0.05$ compared with the PESA40. All data represent the mean value \pm standard deviation ($n = 3$ per group).

There have been no systematic reports on why poly (sodium vinylsulfonate) can improve osteoblast responses. However, some explanations can be found in the literature for why poly (sodium vinylsulfonate) enhances osteoblast responses. Poly (sodium vinylsulfonate) may influence osteoblast behavior through the negatively charged sulfonate groups. The negatively charged sulfonate groups can chelate Ca^{2+} from the surrounding media, a promising feature for transducing osteogenic cues [35]. In addition, the type, quantity, conformation, and activity of absorbed extracellular matrix proteins (e.g., laminin, vitronectin, COL-I, fibronectin, etc.) can be affected by sulfonate groups [36,37], thereby influencing the adhesion, spreading, proliferation, and differentiation of osteoblast. Thus, these explain why poly (sodium vinyl sulfonate) enhances osteoblast responses, although further studies are needed to clarify the underlying mechanism. Previous studies have also confirmed that the sulfonate groups modified surfaces exhibited enhanced in vitro osteogenic activity and in vivo osseointegration [29,30,38–40]. In addition, a high number of sulfonate groups is more beneficial for osteogenic differentiation [41]. The improved proliferation activity of osteoblasts is conducive to more new bone formation around the implant. The ameliorated osteogenic differentiation activity of osteoblasts is conducive to the faster maturation of peri-implant new bone. As a result, enhanced osseointegration is expected in vivo [42]. Therefore, PEEK implants grafted with poly (sodium vinyl sulfonate) on their surfaces facilitate better osseointegration in vivo.

4. Conclusions

In summary, we developed a poly (sodium vinylsulfonate)-functionalized PEEK surface by a one-step and simple UV-induced graft polymerization. Different amounts of poly (sodium vinylsulfonate) were grafted onto the PEEK surface by changing the UV irradiation

time without altering the surface topography and roughness. Poly (sodium vinylsulfonate)-grafted PEEK surfaces, particularly the poly (sodium vinylsulfonate)-grafted PEEK surface obtained after 90 min of UV-induced grafting, can boost the cytocompatibility and osteogenic activity of MC3T3-E1 osteoblast. Subsequent studies will be centered on the underlying mechanism of poly (sodium vinylsulfonate)-grafted PEEK implants enhancing in vitro osteogenic activity of osteoblast and the osseointegration capability in vivo. These findings indicate that PEEK implants grafted with poly (sodium vinyl sulfonate) on the surface have great potential for orthopedic applications.

Author Contributions: Conceptualization, L.L. and Y.Z.; Funding acquisition, L.L. and Y.Z.; Investigation, W.Z. and C.H.; Methodology, L.L. and J.D.; Validation, W.Z., C.H. and Y.L.; Writing—original draft, L.L., J.D., W.Z. and C.H.; Writing—review & editing, L.L. and Y.Z. All authors have read and agreed to the published version of the manuscript.

Funding: This work was supported financially by the Innovation Young Plant Project of Sichuan Province Science and Technology (No. 2018024), the Sichuan Science and Technology Program (No. 2022YFSY0043), the Natural Science Foundation of Sichuan Province (No. 2022NSFSC1537), and the project from Nanchong Science and Technology Project (No. 20SXQT0302).

Institutional Review Board Statement: Not applicable.

Informed Consent Statement: Not applicable.

Data Availability Statement: All data included in this study are available upon request by contact with the corresponding author.

Conflicts of Interest: The authors declare no conflict of interest.

References

1. Wang, Q.; Zhou, P.; Liu, S.; Attarilar, S.; Ma, R.L.W.; Zhong, Y.; Wang, L. Multi-scale surface treatments of titanium implants for rapid osseointegration: A review. *Nanomaterials* **2020**, *10*, 1244. [[CrossRef](#)] [[PubMed](#)]
2. Liu, Y.; Rath, B.; Tingart, M.; Eschweiler, J. Role of implants surface modification in osseointegration: A systematic review. *J. Biomed. Mater. Res. A* **2020**, *108*, 470–484. [[CrossRef](#)] [[PubMed](#)]
3. Qin, L.; Yao, S.; Zhao, J.; Zhou, C.; Oates, T.W.; Weir, M.D.; Wu, J.; Xu, H.H.K. Review on Development and Dental Applications of Polyetheretherketone-Based Biomaterials and Restorations. *Materials* **2021**, *14*, 408. [[CrossRef](#)]
4. He, M.; Huang, Y.; Xu, H.; Feng, G.; Liu, L.; Li, Y.; Sun, D.; Zhang, L. Modification of polyetheretherketone implants: From enhancing bone integration to enabling multi-modal therapeutics. *Acta Biomater.* **2021**, *129*, 18–32. [[CrossRef](#)] [[PubMed](#)]
5. Liu, L.; Zheng, Y.; Zhang, L.; Xiong, C. Bioactive Polyetheretherketone Implant Composites for Hard Tissue. *Prog. Chem.* **2017**, *29*, 450–458.
6. Mishra, S.; Chowdhary, R. PEEK materials as an alternative to titanium in dental implants: A systematic review. *Clin. Implant Dent. R* **2019**, *21*, 208–222. [[CrossRef](#)]
7. Buck, E.; Li, H.; Cerruti, M. Surface Modification Strategies to Improve the Osseointegration of Poly(etheretherketone) and Its Composites. *Macromol. Biosci.* **2020**, *20*, 1900271. [[CrossRef](#)]
8. Verma, S.; Sharma, N.; Kango, S.; Sharma, S. Developments of PEEK (Polyetheretherketone) as a biomedical material: A focused review. *Eur. Polym. J.* **2021**, *147*, 110295. [[CrossRef](#)]
9. Zhang, J.; Wei, W.; Yang, L.; Pan, Y.; Wang, X.; Wang, T.; Tang, S.; Yao, Y.; Hong, H.; Wei, J. Stimulation of cell responses and bone ingrowth into macro-microporous implants of nano-bioglass/polyetheretherketone composite and enhanced antibacterial activity by release of hinokitiol. *Colloid Surf. B* **2018**, *164*, 347–357. [[CrossRef](#)]
10. Yu, X.; Yao, S.; Chen, C.; Wang, J.; Li, Y.; Wang, Y.; Khademhosseini, A.; Wan, J.; Wu, Q. Preparation of Poly(ether-etherketone)/Nanohydroxyapatite Composites with Improved Mechanical Performance and Biointerfacial Affinity. *ACS Omega* **2020**, *5*, 29398–29406. [[CrossRef](#)]
11. Ma, R.; Tang, S.; Tan, H.; Qian, J.; Lin, W.; Wang, Y.; Liu, C.; Wei, J.; Tang, T. Preparation, Characterization, In Vitro Bioactivity, and Cellular Responses to a Polyetheretherketone Bioactive Composite Containing Nanocalcium Silicate for Bone Repair. *ACS Appl. Mater. Interfaces* **2014**, *6*, 12214–12225. [[CrossRef](#)] [[PubMed](#)]
12. Rahmati, M.; Silva, E.A.; Reseland, J.E.; Heyward, A.C.; Haugen, H.J. Biological responses to physicochemical properties of biomaterial surface. *Chem. Soc. Rev.* **2020**, *49*, 5178–5224. [[CrossRef](#)] [[PubMed](#)]
13. Wen, J.; Lu, T.; Wang, X.; Xu, L.; Wu, Q.; Pan, H.; Wang, D.; Liu, X.; Jiang, X. In Vitro and in Vivo Evaluation of Silicate-Coated Polyetheretherketone Fabricated by Electron Beam Evaporation. *ACS Appl. Mater. Interfaces* **2016**, *8*, 13197–13206. [[CrossRef](#)] [[PubMed](#)]

14. Zhu, C.; He, M.; Mao, L.; Li, T.; Zhang, L.; Liu, L.; Feng, G.; Song, Y. Titanium-interlayer mediated hydroxyapatite coating on polyetheretherketone: A prospective study in patients with single-level cervical degenerative disc disease. *J. Transl. Med.* **2021**, *19*, 14. [\[CrossRef\]](#)
15. Ren, Y.; Sikder, P.; Lin, B.; Bhaduri, S.B. Microwave assisted coating of bioactive amorphous magnesium phosphate (AMP) on polyetheretherketone (PEEK). *Mater. Sci. Eng. C* **2018**, *85*, 107–113. [\[CrossRef\]](#)
16. Frankenberger, T.; Graw, C.L.; Engel, N.; Gerber, T.; Frerich, B.; Dau, M. Sustainable Surface Modification of Polyetheretherketone (PEEK) Implants by Hydroxyapatite/Silica Coating—An In Vivo Animal Study. *Materials* **2021**, *14*, 4589. [\[CrossRef\]](#)
17. Zheng, Y.; Xiong, C.; Zhang, S.; Li, X.; Zhang, L. Bone-like apatite coating on functionalized poly(etheretherketone) surface via tailored silanization layers technique. *Mater. Sci. Eng. C* **2015**, *55*, 512–523. [\[CrossRef\]](#)
18. Velard, F.; Braux, J.; Amedee, J.; Laquerriere, P. Inflammatory cell response to calcium phosphate biomaterial particles: An overview. *Acta Biomater.* **2013**, *9*, 4956–4963. [\[CrossRef\]](#)
19. Kassick, A.J.; Yerneni, S.S.; Gottlieb, E.; Cartieri, F.; Peng, Y.; Mao, G.; Kharlamov, A.; Miller, M.C.; Xu, C.; Oh, M.; et al. Osteoconductive Enhancement of Polyether Ether Ketone: A Mild Covalent Surface Modification Approach. *ACS Appl. Bio Mater.* **2018**, *1*, 1047–1055. [\[CrossRef\]](#)
20. Zheng, Y.; Liu, L.; Xiong, C.; Zhang, L. Enhancement of bioactivity on modified polyetheretherketone surfaces with –COOH, –OH and –PO₄H₂ functional groups. *Mater. Lett.* **2018**, *213*, 84–87. [\[CrossRef\]](#)
21. Zheng, Y.; Xiong, C.; Li, X.; Zhang, L. Covalent attachment of cell-adhesive peptide Gly-Arg-Gly-Asp (GRGD) to poly(etheretherketone) surface by tailored silanization layers technique. *Appl. Surf. Sci.* **2014**, *320*, 93–101. [\[CrossRef\]](#)
22. Zhou, T.; Zhu, Y.; Li, X.; Liu, X.; Yeung, K.W.K.; Wu, S.; Wang, X.; Cui, Z.; Yang, X.; Chu, P.K. Surface functionalization of biomaterials by radical polymerization. *Prog. Mater. Sci.* **2016**, *83*, 191–235. [\[CrossRef\]](#)
23. Flejszar, M.; Chmielarz, P. Surface Modifications of Poly(Ether Ether Ketone) via Polymerization Methods-Current Status and Future Prospects. *Materials* **2020**, *13*, 999. [\[CrossRef\]](#) [\[PubMed\]](#)
24. Chouwatat, P.; Hirai, T.; Higaki, K.; Higaki, Y.; Sue, H.-J.; Takahara, A. Aqueous lubrication of poly(etheretherketone) via surface-initiated polymerization of electrolyte monomers. *Polymer* **2017**, *116*, 549–555. [\[CrossRef\]](#)
25. Yousaf, A.; Farrukh, A.; Oluz, Z.; Tuncel, E.; Duran, H.; Dogan, S.Y.; Tekinay, T.; Rehman, H.U.; Yameen, B. UV-light assisted single step route to functional PEEK surfaces. *React. Funct. Polym.* **2014**, *83*, 70–75. [\[CrossRef\]](#)
26. Kyomoto, M.; Moro, T.; Yamane, S.; Watanabe, K.; Takatori, Y.; Tanaka, S.; Ishihara, K. Smart PEEK modified by self-initiated surface graft polymerization for orthopedic bearings. *Reconstr. Rev.* **2014**, *4*, 36–45.
27. Zheng, Y.; Liu, L.; Xiao, L.; Zhang, Q.; Liu, Y. Enhanced osteogenic activity of phosphorylated polyetheretherketone via surface-initiated grafting polymerization of vinylphosphonic acid. *Colloid Surf. B* **2019**, *173*, 591–598. [\[CrossRef\]](#)
28. Liu, L.; Zheng, Y.; Zhang, Q.; Yu, L.; Hu, Z.; Liu, Y. Surface phosphonation treatment shows dose-dependent enhancement of the bioactivity of polyetheretherketone. *RSC Adv.* **2019**, *9*, 30076–30086. [\[CrossRef\]](#)
29. Liu, L.; Zhang, W.; Yuan, L.; Liu, Y.; Zheng, Y. Ameliorative antibacterial, anti-inflammatory, and osteogenic activity of sulfonate-bearing polyetheretherketone toward orthopedic and dental implants. *Mater. Lett.* **2021**, *305*, 130774. [\[CrossRef\]](#)
30. Zheng, Y.; Liu, L.; Ma, Y.; Xiao, L.; Liu, Y. Enhanced Osteoblasts Responses to Surface-Sulfonated Polyetheretherketone via a Single-Step Ultraviolet-Initiated Graft Polymerization. *Ind. Eng. Chem. Res.* **2018**, *57*, 10403–10410. [\[CrossRef\]](#)
31. Zheng, Y.; Xiong, C.; Zhang, D.; Zhang, L. In vitro bioactivity evaluation of α -calcium sulphate hemihydrate and bioactive glass composites for their potential use in bone regeneration. *Bull. Mater. Sci.* **2018**, *41*, 59. [\[CrossRef\]](#)
32. Hao, L.; Fu, X.; Li, T.; Zhao, N.; Shi, X.; Cui, F.; Du, C.; Wang, Y. Surface chemistry from wettability and charge for the control of mesenchymal stem cell fate through self-assembled monolayers. *Colloid Surf. B* **2016**, *148*, 549–556. [\[CrossRef\]](#) [\[PubMed\]](#)
33. Zheng, Y.; Xiong, C.; Wang, Z.; Zhang, L. Enhanced osteoblast cells adhesion, spreading, and proliferation to surface-carboxylated poly(etheretherketone). *J. Bioact. Compat. Pol.* **2015**, *30*, 302–318. [\[CrossRef\]](#)
34. Fan, L.; Guan, P.; Xiao, C.; Wen, H.; Wang, Q.; Liu, C.; Luo, Y.; Ma, L.; Tan, G.; Yu, P.; et al. Exosome-functionalized polyetheretherketone-based implant with immunomodulatory property for enhancing osseointegration. *Bioact. Mater.* **2021**, *6*, 2754–2766. [\[CrossRef\]](#)
35. Wagner, A.-S.; Glenske, K.; Wolf, V.; Fietz, D.; Mazurek, S.; Hanke, T.; Moritz, A.; Arnhold, S.; Wenisch, S. Osteogenic differentiation capacity of human mesenchymal stromal cells in response to extracellular calcium with special regard to connexin 43. *Ann. Anat.* **2017**, *209*, 18–24. [\[CrossRef\]](#) [\[PubMed\]](#)
36. Keselowsky, B.G.; Collard, D.M.; García, A.J. Surface chemistry modulates focal adhesion composition and signaling through changes in integrin binding. *Biomaterials* **2004**, *25*, 5947–5954. [\[CrossRef\]](#)
37. Keselowsky, B.G.; Collard, D.M.; García, A.J. Surface chemistry modulates fibronectin conformation and directs integrin binding and specificity to control cell adhesion. *J. Biomed. Mater. Res. A* **2003**, *66*, 247–259. [\[CrossRef\]](#)
38. Vaquette, C.; Viateau, V.; Guérard, S.; Anagnostou, F.; Manassero, M.; Castner, D.G.; Migonney, V. The effect of polystyrene sodium sulfonate grafting on polyethylene terephthalate artificial ligaments on in vitro mineralisation and in vivo bone tissue integration. *Biomaterials* **2013**, *34*, 7048–7063. [\[CrossRef\]](#)
39. Alcheikh, A.; Pavon-Djavid, G.; Helary, G.; Petite, H.; Migonney, V.; Anagnostou, F. PolyNaSS grafting on titanium surfaces enhances osteoblast differentiation and inhibits Staphylococcus aureus adhesion. *J. Mater. Sci. M* **2013**, *24*, 1745–1754. [\[CrossRef\]](#)
40. Hélar, G.; Noircière, F.; Maying, J.; Migonney, V. A new approach to graft bioactive polymer on titanium implants: Improvement of MG 63 cell differentiation onto this coating. *Acta Biomater.* **2009**, *5*, 124–133. [\[CrossRef\]](#)

-
41. Chaterji, S.; Gemeinhart, R.A. Enhanced osteoblast-like cell adhesion and proliferation using sulfonate-bearing polymeric scaffolds. *J. Biomed. Mater. Res. A* **2007**, *83*, 990–998. [[CrossRef](#)] [[PubMed](#)]
 42. Zhao, Y.; Wong, H.M.; Wang, W.; Li, P.; Xu, Z.; Chong, E.Y.; Yan, C.H.; Yeung, K.W.; Chu, P.K. Cytocompatibility, osseointegration, and bioactivity of three-dimensional porous and nanostructured network on polyetheretherketone. *Biomaterials* **2013**, *34*, 9264–9277. [[CrossRef](#)] [[PubMed](#)]